

Folate-Modified Photoelectric Responsive Polymer Microarray as Bionic Artificial Retina to Restore Visual Function

Zheng-Hang Yu^{1, ‡}, Wei-Jian Chen^{1, ‡}, Xi Liu^{2,3, ‡}, Qiu-Yu Xia¹, Yi-Nuo Yang^{2,3},

Mei Dong¹, Jia-Hao Liu¹, Huai-Jin Guan^{2,3}, Cheng Sun^{2*}, Fu-De Feng^{1*}, Qun-*

Dong Shen^{1}*

1 Department of Polymer Science & Engineering and Key Laboratory of High Performance Polymer Materials & Technology of MOE, School of Chemistry & Chemical Engineering, Nanjing University, Nanjing 210023, China. E-mail: qdshen@nju.edu.cn; fengfd@nju.edu.cn

2 Key Laboratory for Neuroregeneration of Jiangsu Province and Ministry of Education, Co-innovation Center of Neuroregeneration, Nantong University, Nantong 226001, China. Email: suncheng1975@ntu.edu.cn

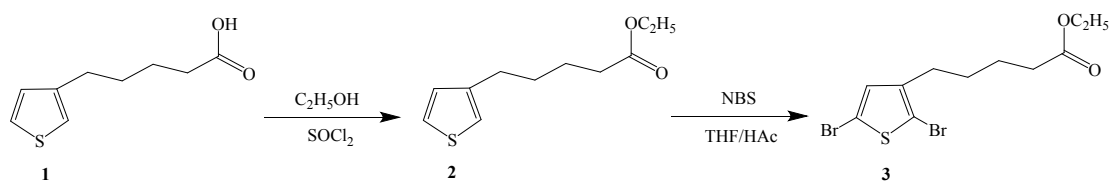
3 Eye Institute, Affiliated Hospital of Nantong University, Nantong 226001, China. E-mail: guanhjeye@163.com

Methods

All of chemicals were purchased from commercial sources and used as received unless otherwise stated. NMR spectra were measured on a Bruker DPX-400 spectrometer. GPC analysis was run on a Shimadzu LC20 AD liquid chromatography system equipped with a RID-20A differential refractive index detector against monodisperse polystyrene standards. THF was used as the eluent at a flow rate of 1.0 mL min⁻¹.

Synthesis of Monomer. Details of synthesis and characterization of monomer was provided in the Figures S1.

The compound 5-(3-thienyl)pentanoic acid (compound 1) was synthesized according to previous report¹.



Compound 1 (3.68 g, 20 mmol) was added to 50 mL of ethanol containing a few drops of SOCl₂ in a 250 mL flask. The mixture was stirred for 24 h at room temperature. After evaporation of solvent under vacuum, the residue was purified by flash chromatography on silica gel using hexane/ethyl acetate (80/20) as eluent to afford ethyl 5-(thiophen-3-yl)pentanoate (compound 2, 3.82 g, 18 mmol). Yield: 90%. ¹H NMR (400 MHz, CDCl₃): δ (ppm) 7.32 – 7.12 (m, 1H), 6.92 (d, J = 4.3 Hz, 2H), 4.12 (q, J = 7.1 Hz, 2H), 2.65 (d, J = 6.9 Hz, 2H), 2.32 (t, J = 6.5 Hz, 2H), 1.76 – 1.55 (m, 4H), 1.24 (t, J = 7.0 Hz, 3H); ¹³C NMR (100 MHz, CDCl₃): δ (ppm) 173.62, 142.45, 128.17, 125.27, 120.07, 60.45, 60.25, 34.35, 34.15, 30.00, 29.93, 24.61, 24.43, 14.30.

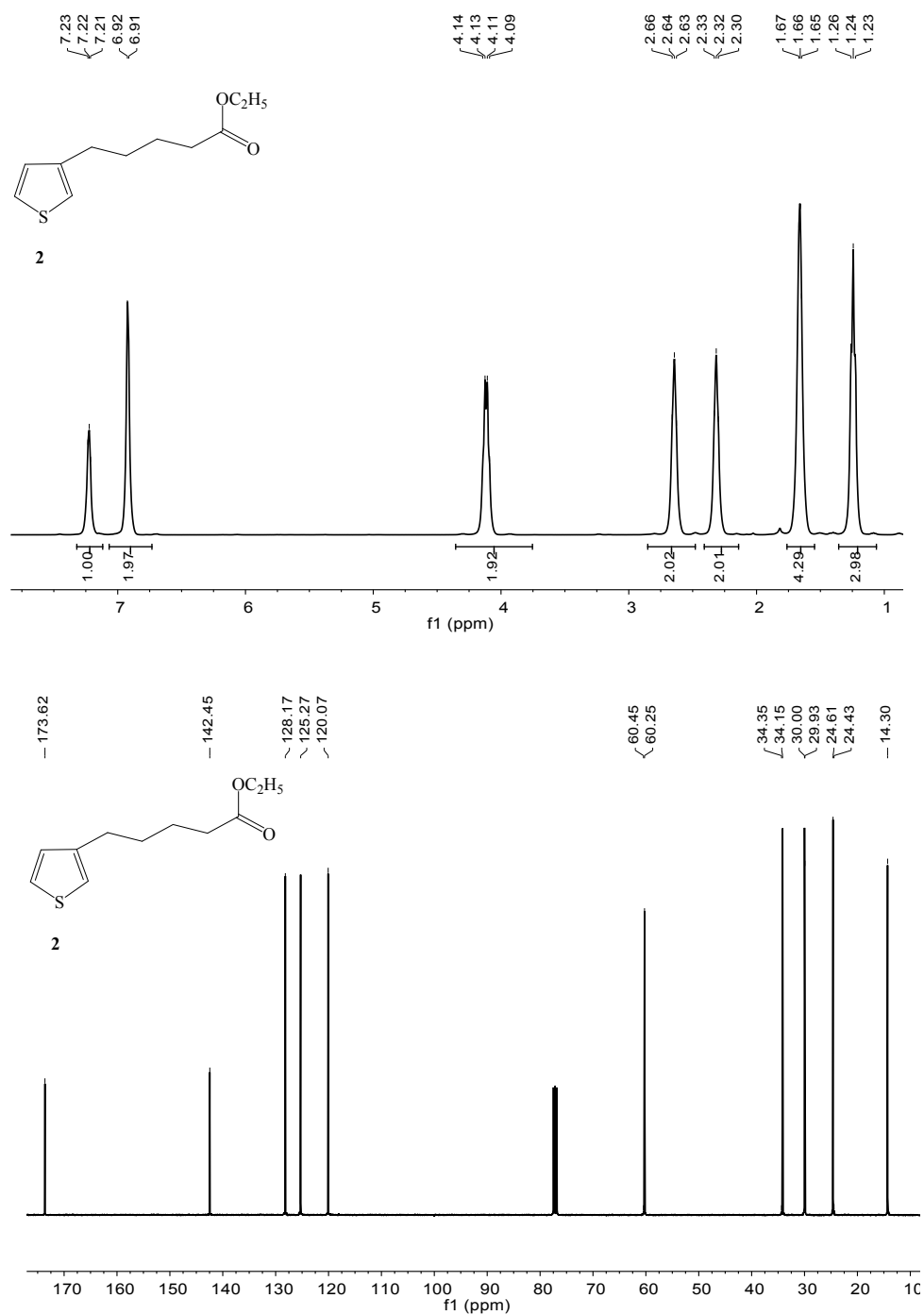


Figure S1. ¹H NMR and ¹³C NMR spectra of compound 2 in CDCl₃.

To a solution of compound 2 (2.12 g, 10 mmol) in THF/CH₃COOH (5 mL/5 mL) was added 2.4 equivalent molar NBS, and the mixture was stirred at room temperature for 2 h. After chloroform (10 mL) was added, the mixture was successively washed with

distilled water and aqueous sodium bicarbonate. The organic layer was dried and concentrated under vacuum. The residue was purified by flash chromatography on silica gel using hexane/ethyl acetate (80/20) as the eluent to afford ethyl 5-(2,5-dibromothiophen-3-yl)pentanoate (compound 3, 3.25 g, 8.8 mmol). Yield: 88%. ^1H NMR (400 MHz, CDCl_3): δ (ppm) 6.78 (s, 1H), 4.13 (q, $J = 7.2$ Hz, 2H), 2.31 - 2.55 (dt, $J = 83.6, 7.3$ Hz, 4H), 1.63 (dp, $J = 23.6, 7.6$ Hz, 4H), 1.26 (t, $J = 7.1$ Hz, 3H); ^{13}C NMR (100 MHz, CDCl_3): δ (ppm) 173.45, 142.25, 130.84, 110.54, 108.63, 108.24, 77.38, 77.26, 77.06, 76.74, 66.71, 66.39, 60.34, 50.00, 34.02, 33.93, 33.52, 29.58, 29.13, 29.01, 28.22, 24.36, 14.29.

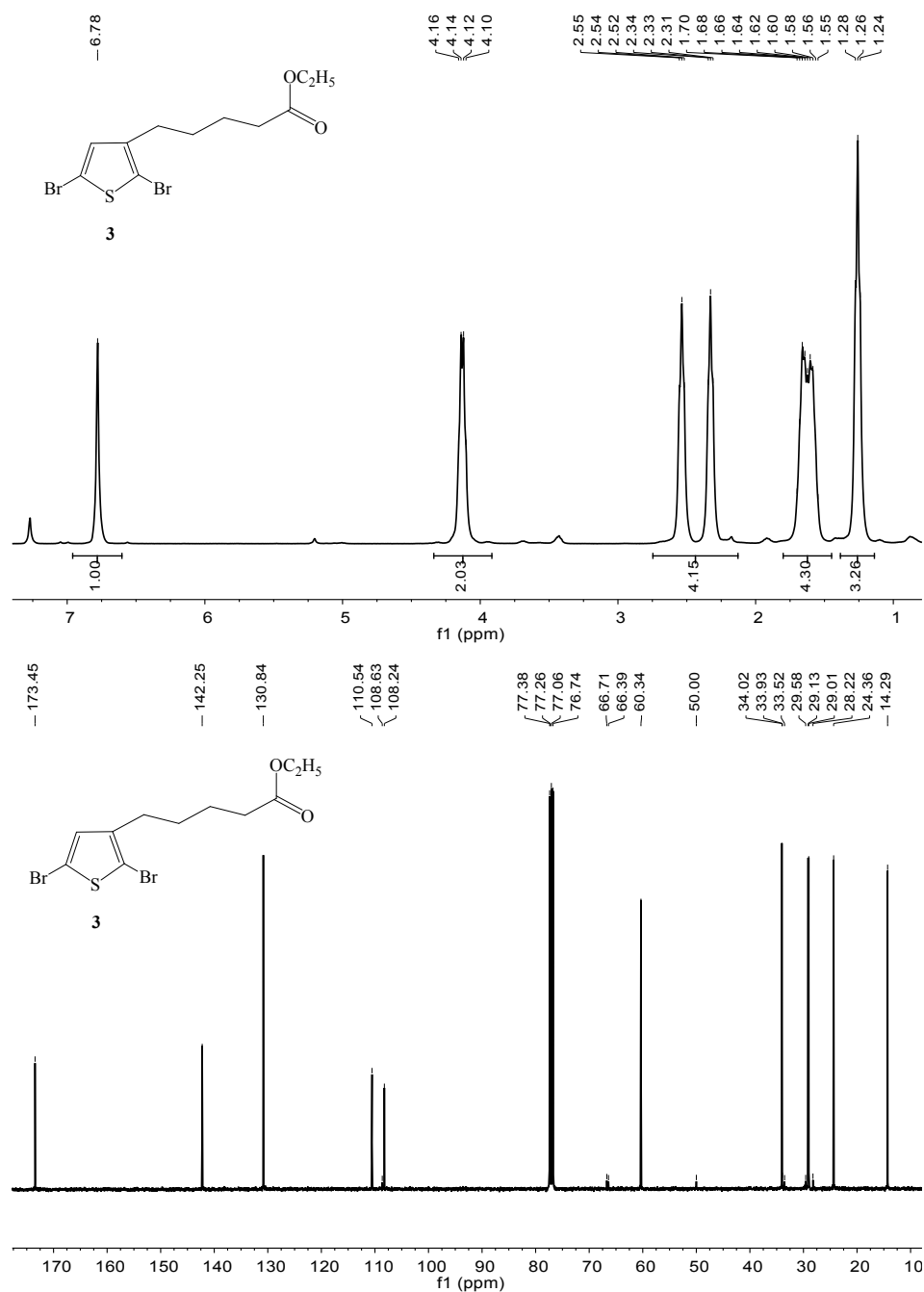


Figure S2. ¹H NMR and ¹³C NMR spectra of compound 3 in CDCl₃.

General Procedure for the Polymerization of Monomer (compound 3):

Monomer (5 mmol) was dissolved in THF (25 mL) and cooled to −40 °C under an argon atmosphere. To this solution was added i-PrMgCl·LiCl (1.3 M in THF, 4.94

mmol) via a syringe over a period of 5 min. The mixture was stirred under argon for 1 h at $-40\text{ }^{\circ}\text{C}$. After quick warming up to $0\text{ }^{\circ}\text{C}$, 20 mL of the solution via a syringe was added into a new flask containing 54.2 mg of $\text{Ni}(\text{dppp})\text{Cl}_2$ (0.1 mmol). The mixture was stirred at $0\text{ }^{\circ}\text{C}$ for 1 h and then quenched by addition of 0.5 mL of 1.0 M aq. HCl. After filtration, solvent was removed under reduced pressure. The residue was redissolved in chloroform, successively washed by aq. NH_4Cl , brine, and water, and dried over anhydrous MgSO_4 to yield an orange solution. After evaporation, multiple methanol precipitation, filtration, and vacuum drying treatments, the polymer products were obtained. GPC (THF): $M_n = 11.8\text{ kDa}$, $d = 1.11$. $^1\text{H NMR}$ (400 MHz, CDCl_3): δ (ppm) 6.78 (s, CH), 4.13 (q, CH_2), 2.31 - 2.55 (dt, CH_2), 1.63 (dp, CH_2), 1.26 (t, CH_3).

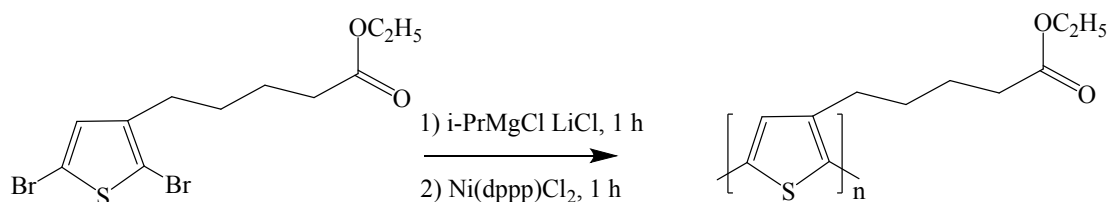


Figure S3. Synthesis of P3EPT

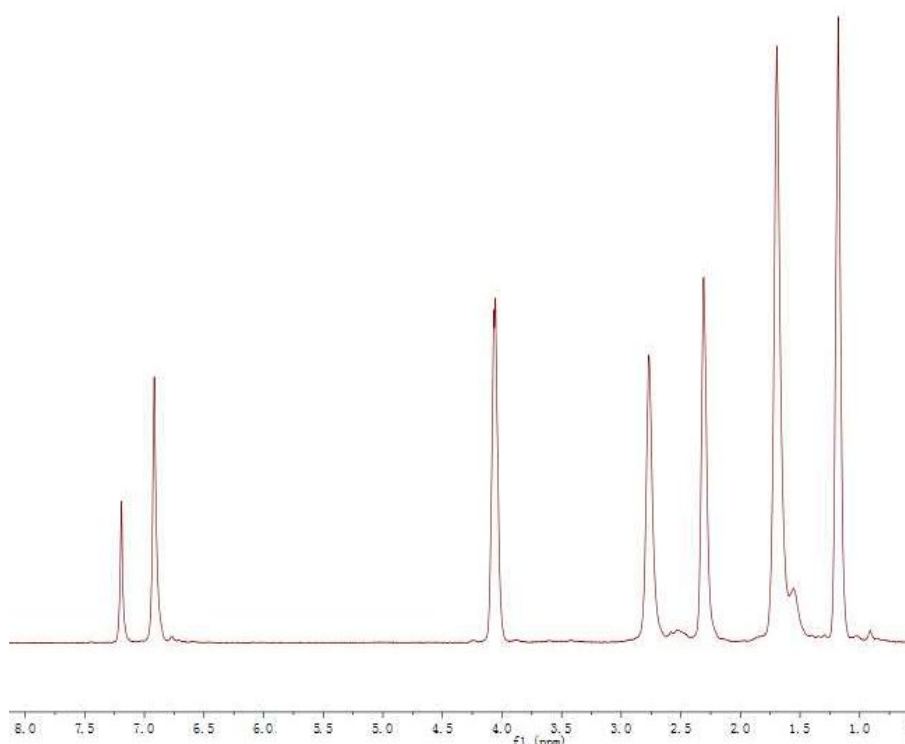


Figure S4. ^1H NMR spectrum of P3EPT in CDCl_3 .

Synthesis of P3EPT-FA:

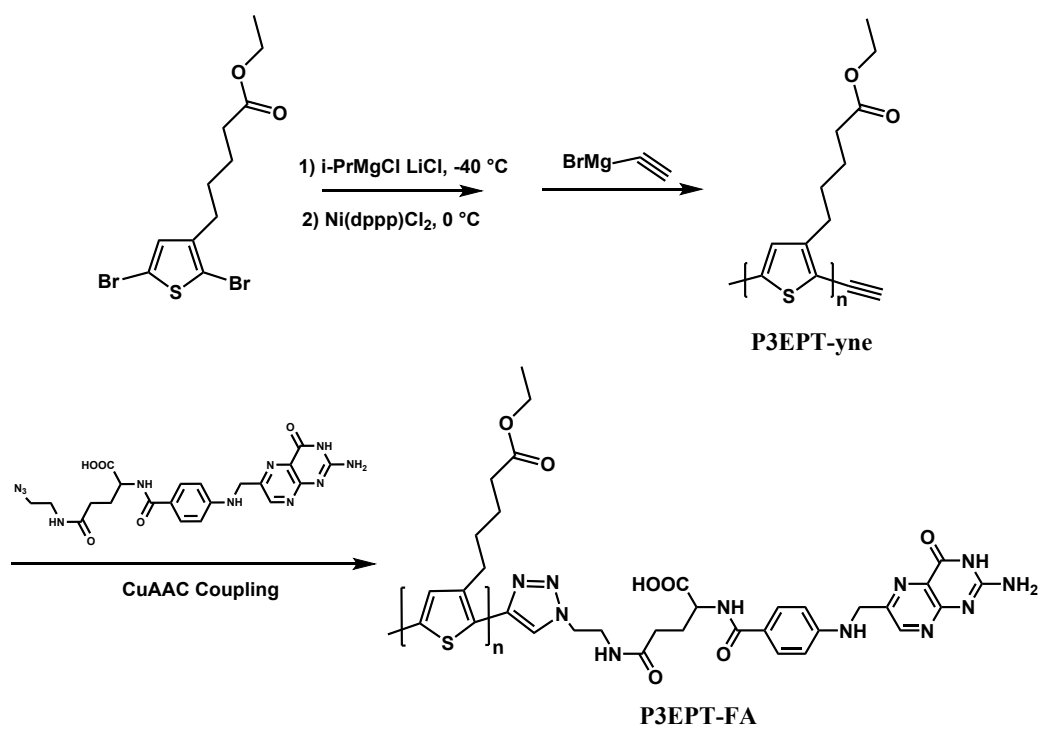


Figure S5. Synthesis of P3EPT-FA.

Figure S6. ^1H NMR spectrum of P3EPT-yne in CDCl_3 .

P3EPT-yne (100 mg, 26.8 μmol) and folate azide² (31.0 mg, 60.0 μmol) were dissolved in a mixture of THF(15 mL) and DMSO (15 mL). Sodium ascorbate (3 mg, 5 μmol) and copper sulfate pentahydrate (1.5 mg, 6 μmol) were added. The reaction mixture was stirred for 48 h at room temperature, and precipitated in methanol. After filtration, the precipitation was washed with DMSO (3 \times 50 mL), distilled water (3 \times 50 mL), and then dried under vacuum to yield P3EPT-FA.

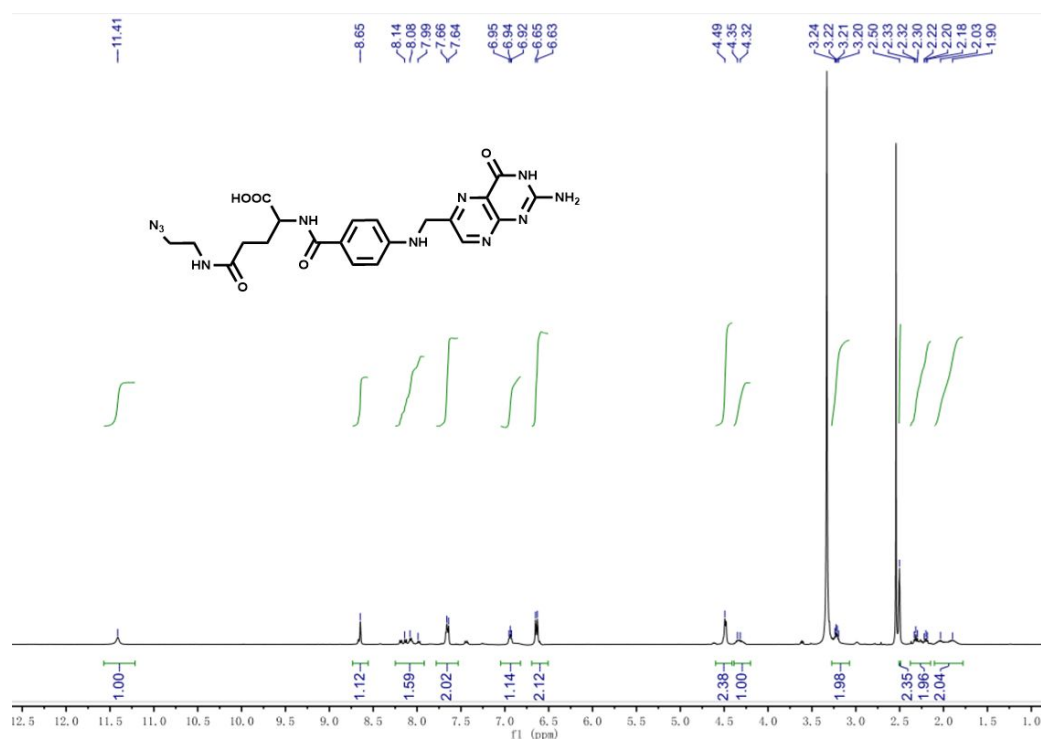


Figure S7. ^1H NMR spectrum of folate-azide in DMSO-d_6 .

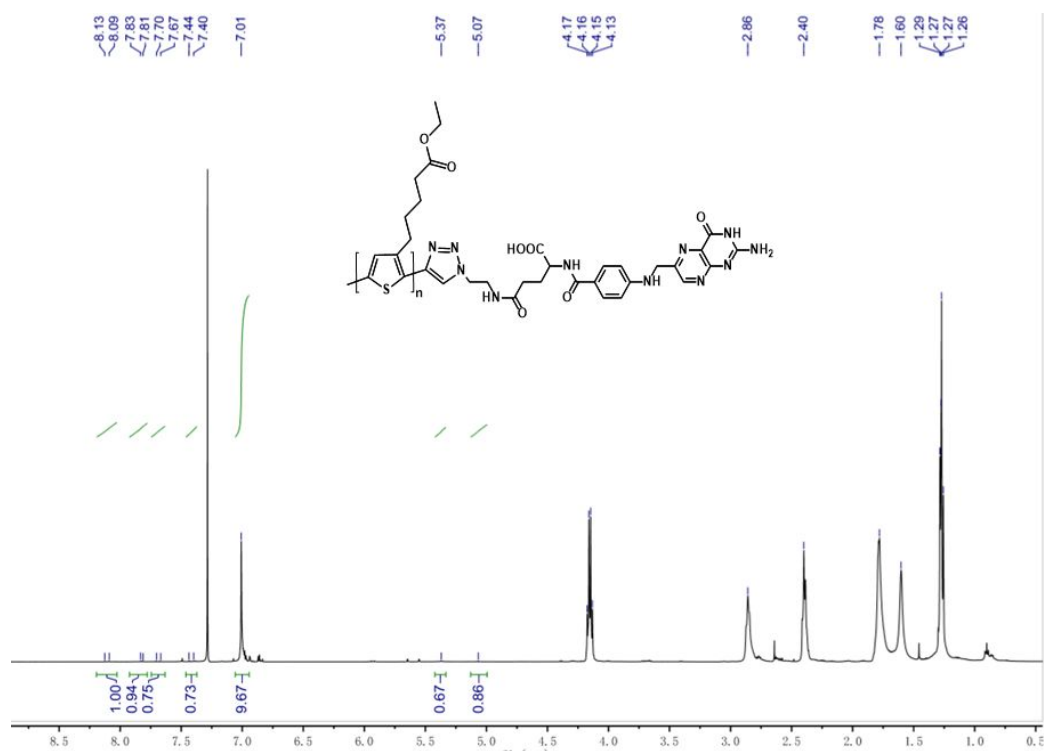


Figure S8. ¹H NMR spectrum of P3EPT-FA in CDCl₃.

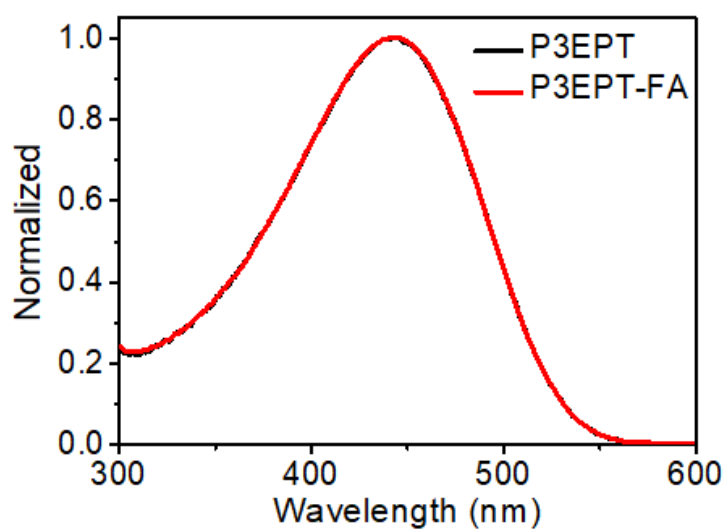


Figure S9. The normalized UV-vis absorption spectra of P3EPT (black line) and P3EPT-FA (red line) in THF solution.

Planar				h	r	θ	S	Array	S
—	14.6	7.3	1556.068	14.6	0	180	0		
P3EPT	15	7.5	22.5	12.43	5.6519996	131.09681	100.35849		117.08491
P3EPT-FA	18.1	9.05	27.15	9.35	9.0450263	91.899656	257.02155		299.85847
Petri dish	20	10	30	8.51	9.888372	81.43102	307.18462		

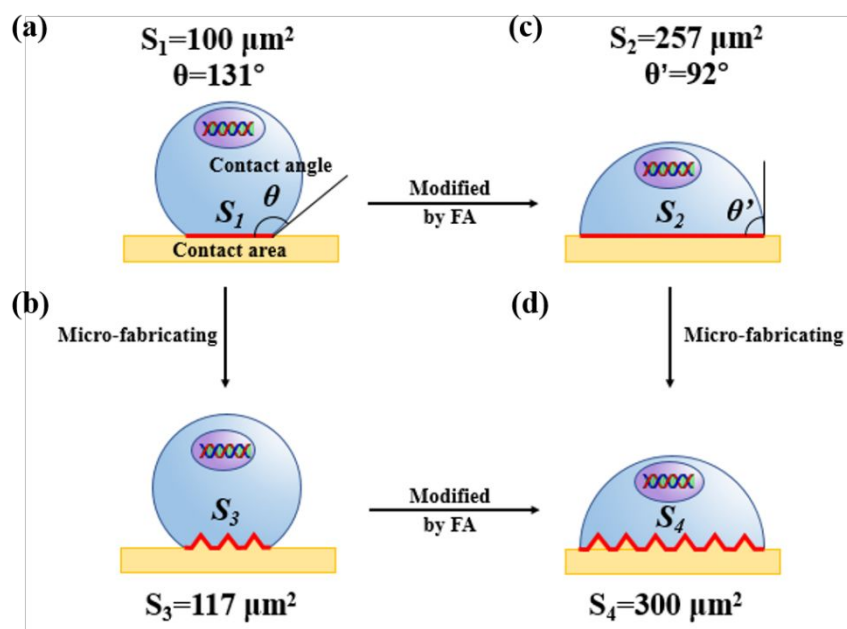


Figure S10. The simulation of contact angles and areas³ between N2A cells and P3EPT (a) planar and (b) array films; P3EPT-FA (c) planar and (d) array films.

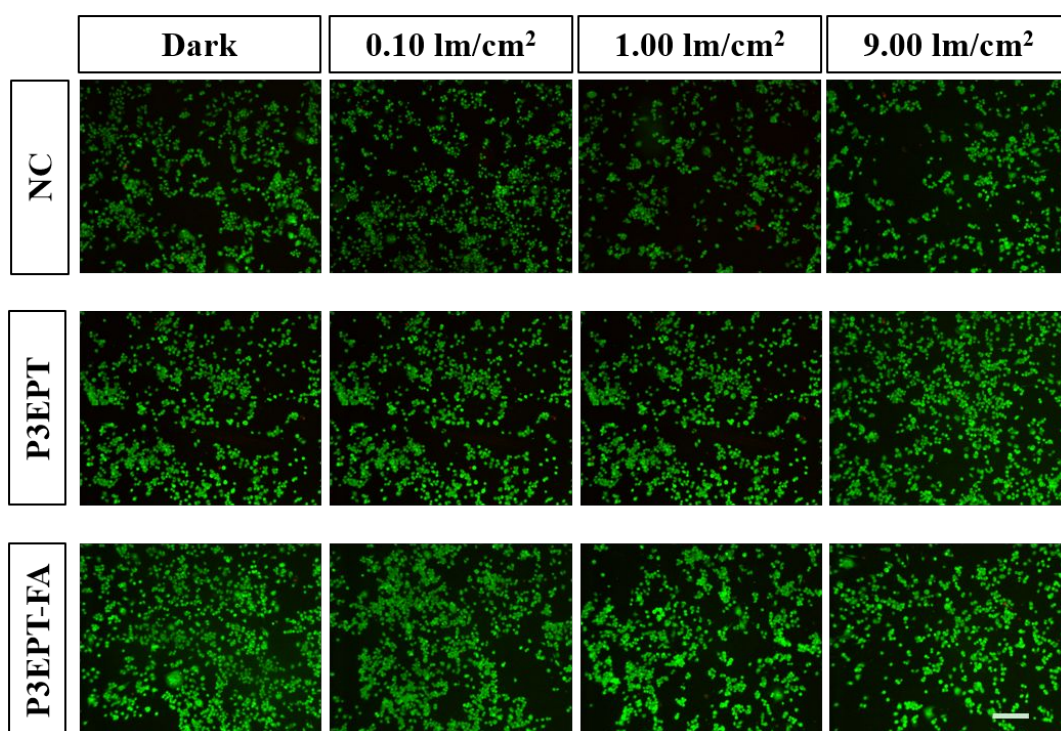


Figure S11. Cellular-viability assessment of N2A cells. The cells were seeded on different substrates under dark or light condition; the scale bar is 50 μm . The cells were stained with AO/PI.

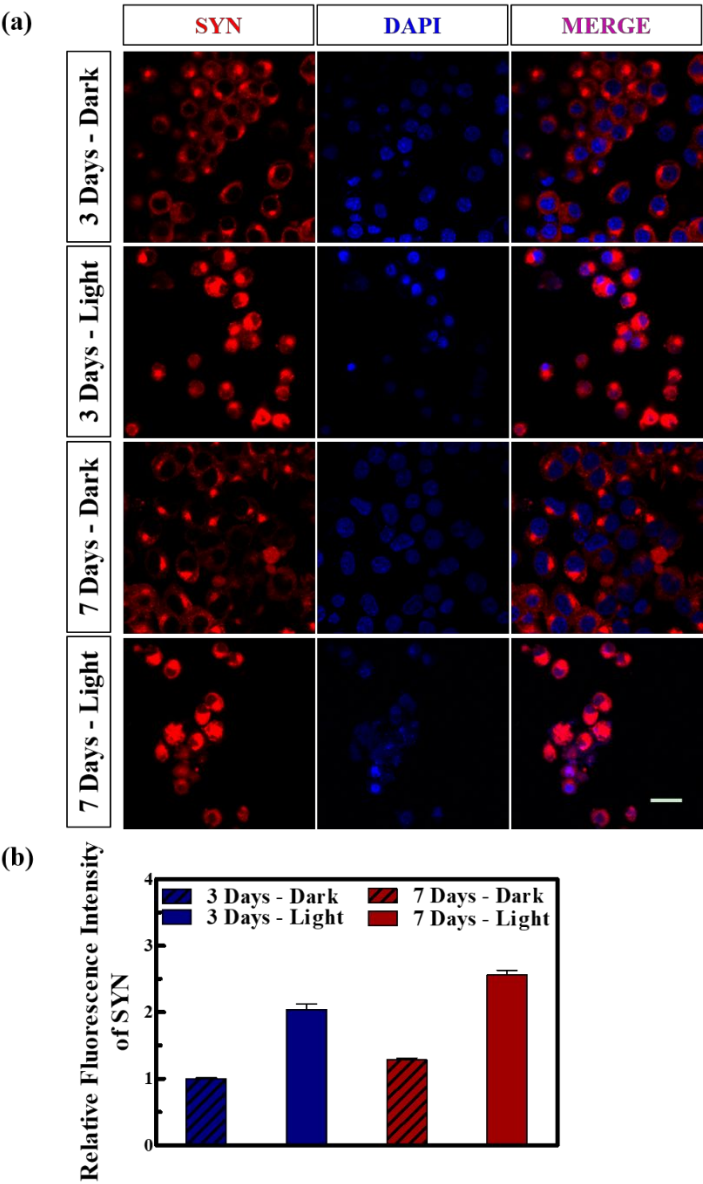


Figure S12. Synaptophysin expression in nerve cells. (a) Immunofluorescence images of SYN in N2A cells; the scale bar is 20 μm . (b) Relative SYN immunofluorescence intensity of the cells in different groups.

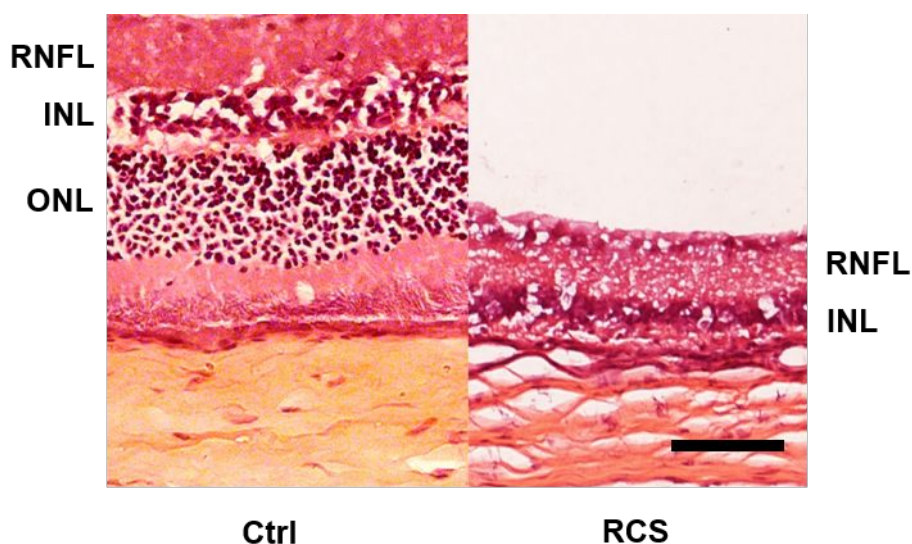


Figure S13. Hematoxylin & eosin-stained histological sections of Sprague-Dawley (SD) rat retina and RCS rat retina. The scale bar denotes 10 μm . RNFL: retinal nerve fiber layer; INL: inner nuclear layer; ONL: outer nuclear layer.

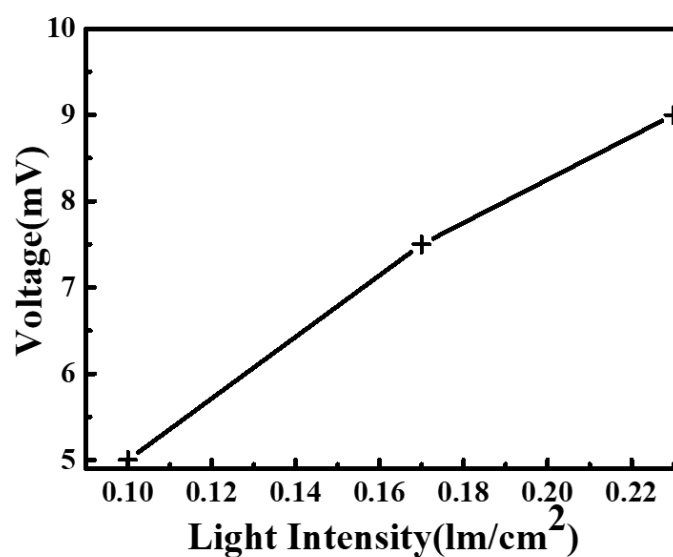


Figure S14. Voltage response curve for the artificial retina illuminated by white LED.

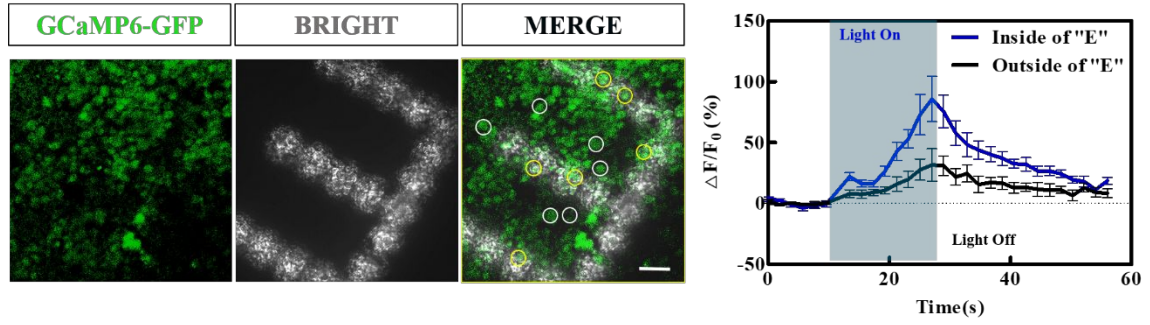


Figure S15. (Left) Fluorescence images of the nerve cells illumination by blue LED with power of 9.00 lm/cm². The scale bar is 50 μ m. (Right panel) Fluorescence traces indicating the change of intracellular calcium ion concentration for the cells under light and in dark (six cells were selected for each group).

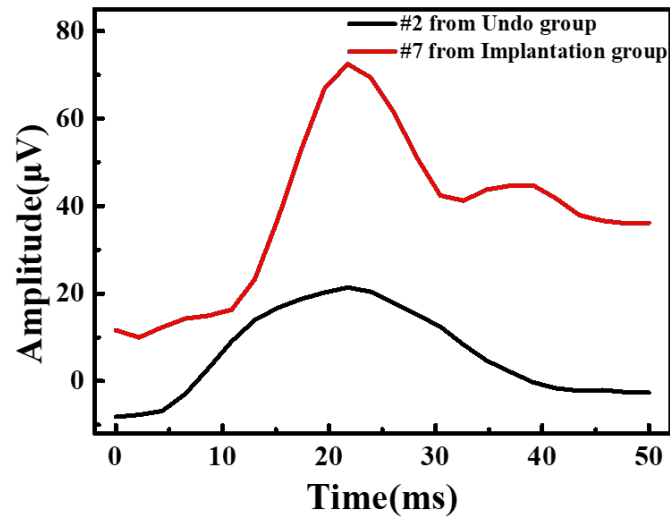


Figure S16. The raw VEP recorded from the animals with and without the prosthesis by an electrophysiological diagnostic system (Roland Consult, Reti-port/ scan21).

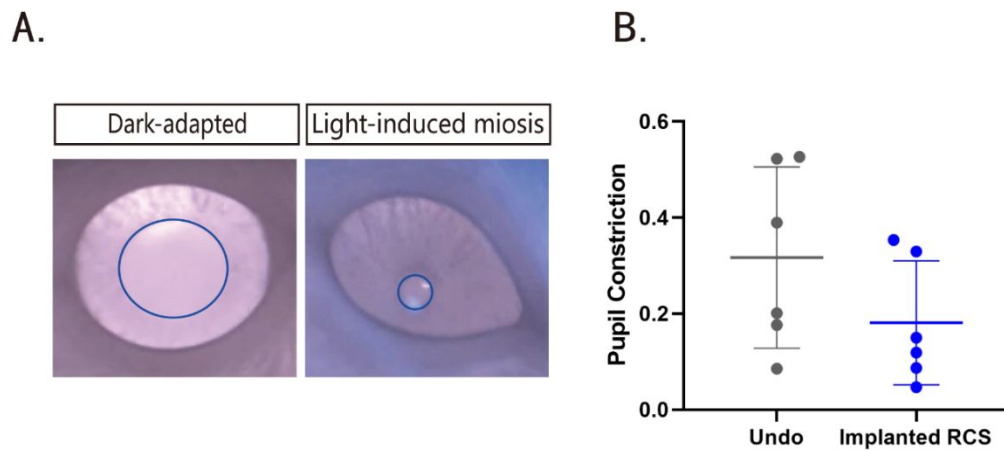


Figure S17. Rescue of the pupillary reflex. A, Constriction of the pupil by light pulses as assessed using standard infrared imaging in the implanted RCS rats. B, The changes of PLR showing a restoring trend in the implanted rats. Pupil constrictions (means \pm SEM) were: undo, 0.32 ± 0.08 (n = 6); implanted RCS rats, 0.18 ± 0.05 (n = 6). Unpaired Student's t test, $p = 0.17$.

Table S1. The original VEP data.

	Eye number	VEP1	VEP2	VEP3	VEP4	VEP5	Average
undo	#1	27.8	63.8	59.6	29.0	57.7	47.58
	#2	23.3	79.0	48.3	52.1	43.5	49.24
	#3	29.5	37.7	15.8	17.5	8.8	21.86
	#4	47.0	42.6	77.4	46.8	47.9	52.34
	#5	90.0	82.2	61.7	51.5	66.0	70.28
	#6	46.1	42.9	51.4	45.8	45.6	46.36
	#7	64.2	53.8	45.3	48.6	47.8	51.94
	#8	62.3	57.1	28.2	95.5	42.2	57.06

	#9	81.9	64.0	30.9	52.3	61.3	58.08
	#10	37.7	35.8	31.7	38.0	58.3	40.30
	#11	49.8	60.8	65.1	41.7	39.6	51.40
RCS	#1	70.8	40.7	67.8	89.3	40.2	61.76
	#2	46.6	45.8	45.4	49.2	383.1	114.02
	#3	81.3	69.5	24.2	33.2	44.3	50.50
	#4	41.1	89.5	83.6	66.9	42.1	64.64
	#5	83.0	44.1	82.6	58.4	76.9	69.00
	#6	146.4	97.9	51.7	64.9	80.0	88.18
	#7	80.7	68.3	77.4	71.9	76.8	75.02
	#8	47.8	85.8	95.0	51.9	76.9	71.48
	#9	107.7	153.9	42.7	62.2	69.3	87.16

* We recorded 5 times for each eye and the average values were used for the final analysis.

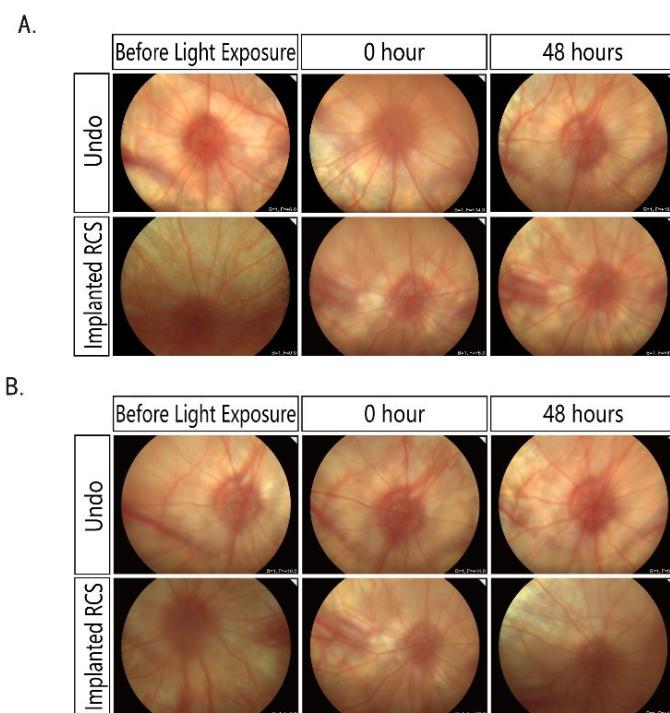


Figure S18. Fundus condition after red and blue light irradiation. A. The condition of the fundus after red light irradiation (1400 lux; 5 min). B. The condition of the fundus after blue light irradiation. The light source was replaced by blue light (1400 lux; 5 min), other conditions are the same as in A.

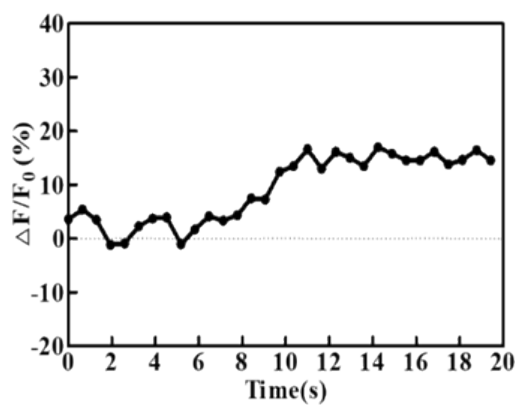


Figure S19. Fluorescence traces indicating the change of intracellular calcium ion concentration for the single cell.

We used albino RCS rats (Figure S20). In the RCS rat model used, degeneration starts at approximately 12 days, and the photoreceptors are completely degenerated by approximately 77 days⁴. So we operated rats at 2-3 months of age. Based on previous explorations and researches on the occurrence and development of retinal degeneration in RCS rats, many RP therapeutic operations were performed around the 21st day after birth⁵⁻⁶. We took into account the above reasons, so we operated at 2-3 months of age.



Figure S20. A photograph of albino RCS rats.

REFERENCES

1. Motiwala, H. F.; Vekariya, R. H.; Aube, J., Intramolecular Friedel-Crafts Acylation Reaction Promoted by 1,1,1,3,3,3-Hexafluoro-2-propanol. *Org Lett* **2015**, *17* (21), 5484-5487.

2. Mishra, K.; Joy, A., Dual Functionalized Telechelic Block Copolymers with Reproducible Block Sizes Prepared by Microwave Assisted RAFT Polymerization. *Polymer* **2015**, *66*, 110-121.
3. Erbil, H. Y., The Debate on the Dependence of Apparent Contact Angles on Drop Contact Area or Three-Phase Contact Line: A Review. *Surface Science Reports* **2014**, *69* (4), 325-365.
4. LaVail, M. M.; Battelle, B. A., Influence of Eye Pigmentation and Light Deprivation on Inherited Retinal Dystrophy in the Rat. *Exp Eye Res* **1975**, *21* (2), 167-192.
5. Ciavatta, V. T.; Mocko, J. A.; Kim, M. K.; Pardue, M. T., Subretinal Electrical Stimulation Preserves Inner Retinal Function in RCS Rat Retina. *Mol Vis* **2013**, *19*, 995-1005.
6. Pardue, M. T.; Phillips, M. J.; Yin, H.; Sippy, B. D.; Webb-Wood, S.; Chow, A. Y.; Ball, S. L., Neuroprotective Effect of Subretinal Implants in the RCS Rat. *Invest Ophthalmol Vis Sci* **2005**, *46* (2), 674-682.